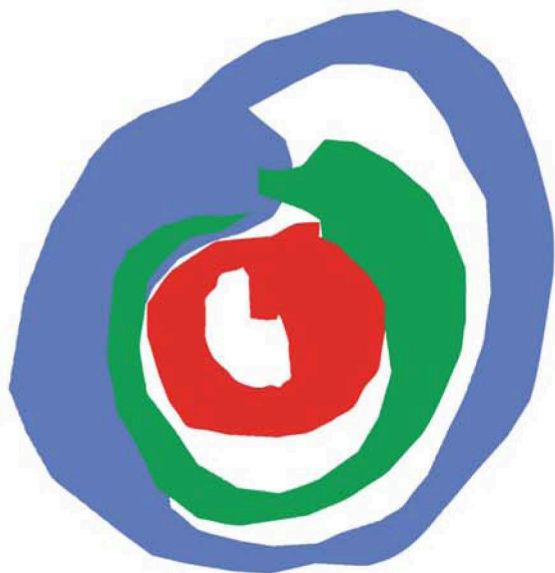


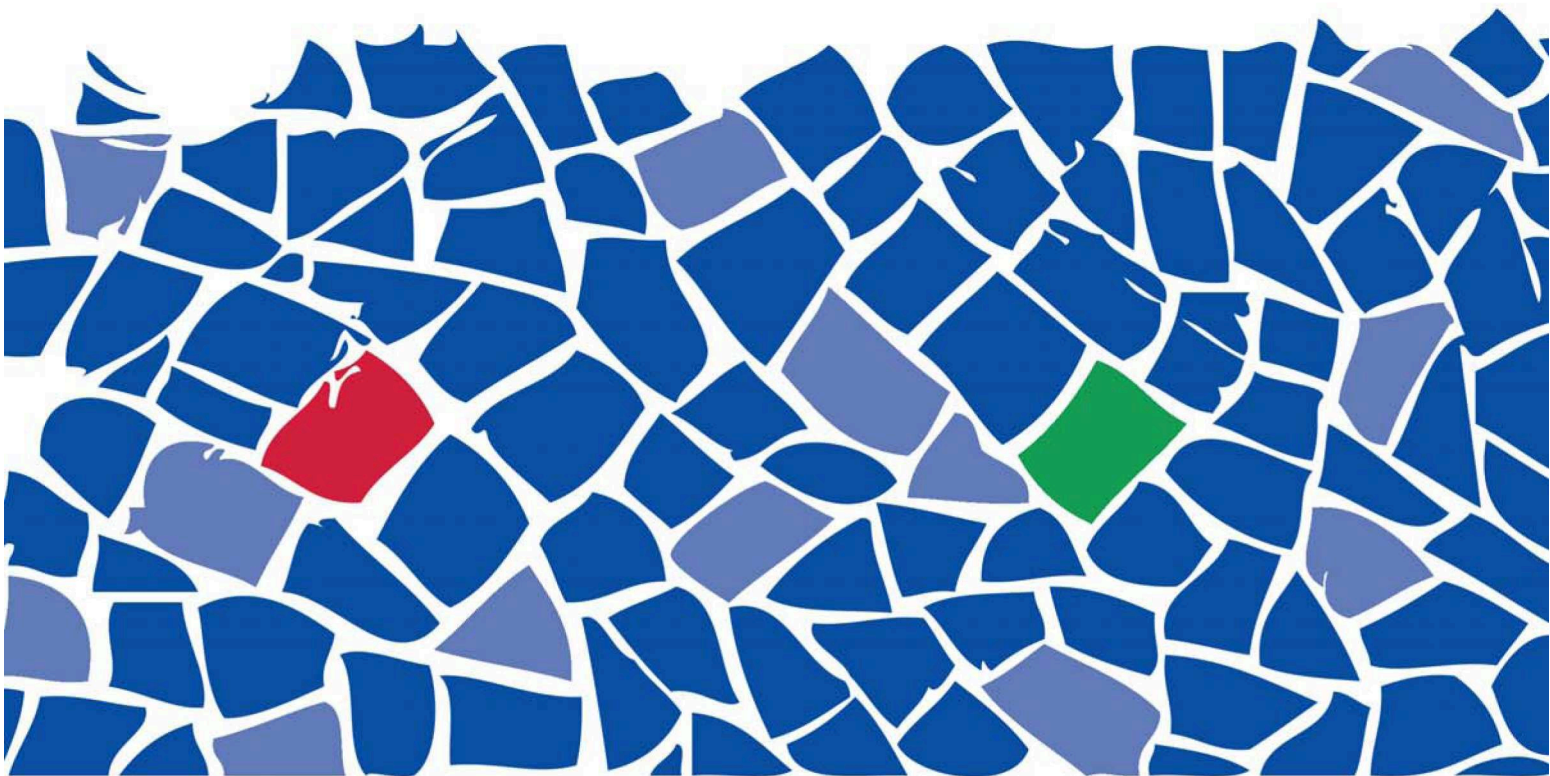
TRANSACTIONS

30 May to 2 June 2010, Palau de Congressos de Catalunya, Barcelona, Spain



EN/C  
2010

EUROPEAN NUCLEAR CONFERENCE



EUROPEAN NUCLEAR SOCIETY



© 2010 European Nuclear Society  
Rue Belliard 65  
1040 Brussels, Belgium  
Phone + 32 2 505 30 54  
Fax +32 2 502 39 02  
E-mail [ens@euronuclear.org](mailto:ens@euronuclear.org)  
Internet [www.euronuclear.org](http://www.euronuclear.org)

---

ISBN 978-92-95064-09-6

These transactions contain all contributions submitted by 28 May 2010.

The content of contributions published in this book reflects solely the opinions of the authors concerned. The European Nuclear Society is not responsible for details published and the accuracy of data presented.



**ENC 2010**  
European Nuclear Conference



## **Poster**

### **Life science applications**

# NUCLEAR EMERGENCY RESPONSE EXERCISES AND DECISION SUPPORT SYSTEMS – INTEGRATING DOMESTIC EXPERIENCE WITH INTERNATIONAL REFERENCE SYSTEMS.

D.S. SLAVNICU, D.V. VAMANU, D. GHEORGHIU, V.T. ACASANDREI  
*'Horia Hulubei' National Institute of Physics and Nuclear Engineering, IFIN-HH  
Atomistilor Street no.407, P.O.BOX MG-6, Bucharest - Magurele, Romania*

E. SLAVNICU  
*Politechnica University of Bucharest  
Splaiul Independentei 313, Building BN 105, 060042, Bucharest, Romania*

## ABSTRACT

The paper glosses on the experience of a research-oriented team routinely involved in emergency preparedness and response management activities, with the assimilation, implementation, and application of decision support systems (DSS) of continental reference in Europe, and the development of supportive, domestic radiological assessment tools. Two exemplary nuclear alert exercises are discussed, along with solutions that emerged during drill planning and execution, to make decision support tools of various origins and strength to work synergistically and complement each other.

## 1. Introduction

The paper aims at drawing attention on several aspects relevant in the decision support-assisted (DSS) management of radiological emergency, with emphasis on the use of alternative and mutually-supportive assessment resources. In May 2005, the *International Atomic Energy Agency* has conducted a comprehensive nuclear alert exercise, code-named ConvEx-3 in an attempt to verify the capability of assessment and reaction to a significant abnormal event in a nuclear facility – the Cernavoda Nuclear Power Plant (Romania). Four years later, AXIOPOLIS 2009 has called together again the plant, the Cernavoda City Hall, the national Nuclear Authority and the topical research to test their strenghts and identify weaknesses in the nuclear emergency management. The major league players in the exercises were RODOS (*Real-Time, On-Line Decision Support System for the Management of Nuclear Emergencies in Europe*) and MOIRA (*A Model-Based Computerised System for Management Support To Identify Optimal Remedial Strategies For Restoring Radionuclide Contaminated Aquatic Ecosystems And Drainage Area*), both developed by multinational consortia within the EU Framework Programmes 4, 5, and 6. In the domestic league, specific roles were allocated to RAT (*Radiological Assessment Toolkit*) – an open-ended software platform of an MS&V (*Modeling, Simulation and Visualization*) profile that assembles requisite source term, environmental transport, dosimetric, dose-effect, and dose/derived intervention level-countermeasure correlated facilities connected to GIS and physical data libraries. The four-year lapse time between the drills have seen the tools evolving as far as state of the art – from standalone to web applications, and status – RODOS being successfully implemented in the *National Centre for Nuclear Accident and Radiological Emergencies* (NCNA), by the original licensee – the *National Institute of Physics and Nuclear Engineering*, Bucharest (IFIN-HH).

## 2. ConvEX-3, at IFIN-HH

From the IFIN-HH perspective, the ConvEX-3 theatre of action was comprised of a) *the RODOS server*, located on the IFIN-HH premises, and the operating team around it; b) *the RODOS remote operator*, on duty at the *National Emergency Response Center*, downtown Bucharest; c) *the RODOS authorized correspondents* abroad; and d) *the technical support team* operating RAT as a RODOS assistant, also at NIPNE. In a first step, the RAT assistants have expeditiously provided 8-hour meteo forecasts emphasizing the wind and precipitation regime at and near the accident site, with a potential coverage of the mesoscale. To this effect, the RAT team has issued a dedicated software capable of offline-browsing a public meteorological forecast data resource – *U.S.A. Weather Channel/UK.Weather.com* in order to mine-out and pre-process parameters of prime consequence in determining the motion and the dispersive properties of masses of air overflowing the Cernavoda NPP area prior, and during the (simulated) abnormal release. The second step was seeing RODOS at work, given the input described. Thus, *Accident's Day-1* had a first release reportedly occurring at 06:30 hours. The source term was provided – if with a considerable delay - by the NPP Cernavoda and consisted of 17 radionuclides: H-3, Kr-83m, Kr-85m, Kr-85, Kr-88, Kr-89, Xe-133m, Xe-133, Xe-135m, Xe-135, Xe-138, I-131, I-132, I-133, I-135, Cs-134, Cs-137 and Cs-138. The meteorological scenario that was imposed by the exercise Organizers for the first hours into the release has presumed that the wind direction is towards the city of Cernavoda, to favor the deployment of intervention forces in the field and the mobilization of the population as a part in the drill. As expected, the first information required by the decision makers has targeted the appropriateness of *early countermeasures* - sheltering and evacuation of population, administration of iodine tablets - and the dose levels expected in the potentially affected area. Figure1 illustrate the doses consecutive to the first round in the (virtual) release, that was assumed to last for 4 hours. Based on this evaluation RODOS recommended the administration of iodine tablets to children, in a specified and charted area. It also concluded that sheltering in a small area surrounding the source of release would be in order, but no evacuation was warranted. The system has also offered evaluations of the radioactivity in the food and feedstock. Based on these results a recommendation was issued – to ban the local milk and diary product consumption in an area 10 km in radius around the NPP. *In the second day of the exercise* a controlled release through the stack was assumed and the true wind direction was taken into account. On these, RODOS had no countermeasure to recommend, as the predicted doses were below the normative levels. In turn, MOIRA recommended the ban of river water use; on the other hand, the predicted concentration of Cs-137 in fish (Figure 2) was below the normative levels, so that no countermeasures were in order. Complementarily, RAT has also engaged in the *radiological assessment* and the *countermeasure design*. However, in contrast with RODOS – that was bearing the prime responsibility for issuing, near-real time manner, information of immediate relevance for directing the response, RAT has adopted a strategy of alternative situations coverage, based on 'what if' scenarios. Figure 3 presents essential countermeasure areas that would follow from RAT assessments conducted as described.

### **3. AXIOPOLIS 2009, at NCNA**

AXIOPOLIS 2009 was a nation-wide drill around a scenario based on a source term delivered by Cernavoda NPP team and consisting of two groups of radionuclides: noble gases (Kr-83m, Kr-85m, Kr-85, Kr-88, Kr-89, Xe-133m, Xe-133, Xe-135m, Xe-135, Xe-138) and iodine ( I-131, I-132, I-133, I-135). Since the RODOS system was already operational in the *National Centre for Nuclear Accident and Radiological Emergencies* (NCNA), the on-the-drill assessment to support decision makers was performed on the very Centre's premises. To make the drill work, however, the RODOS/MOIRA/RAT team at IFIN-HH, Bucharest had

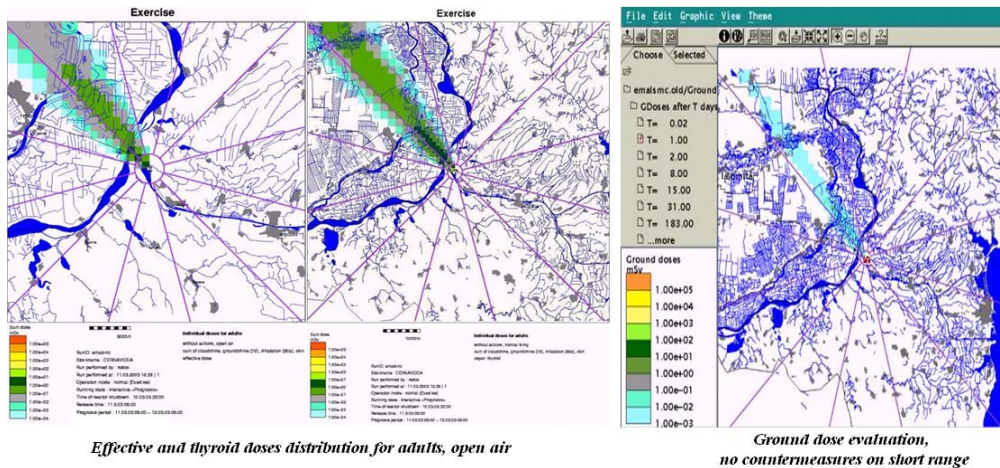


Fig 1. The doses consecutive to the first round in the (virtual) release, for 4 hours.

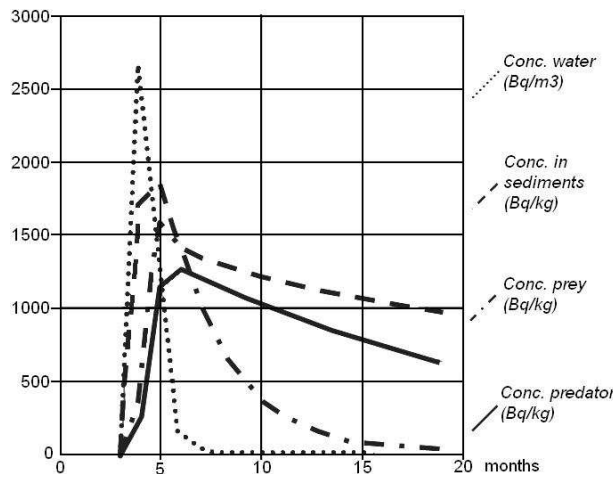


Fig.2 CONVEX- 3. MOIRA results for Cernavoda NPP site, Cs-137 concentration

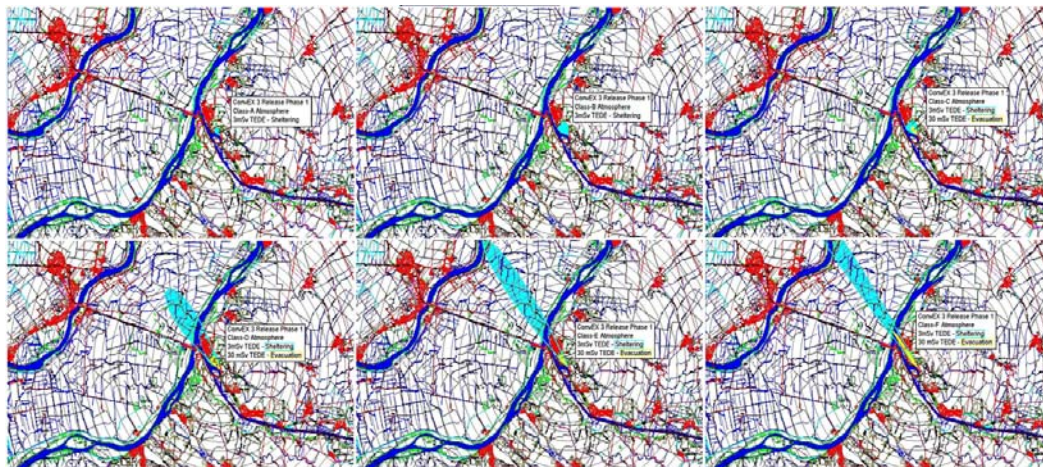


Fig.3. Doses by classes of atmospheric stability (Pasquill A, B, C, D, E, F).

to run, in the planning phase, a considerable number of 'what if' scenarios, and conduct extensive exchanges with the Nuclear Authority (the *National Commission for Nuclear Activity Control – CNCAN*) and the plant emergency managers so as to size a response area ('evac and iodine admin sim') in a scientifically-defendable and ALARA-conscious manner.

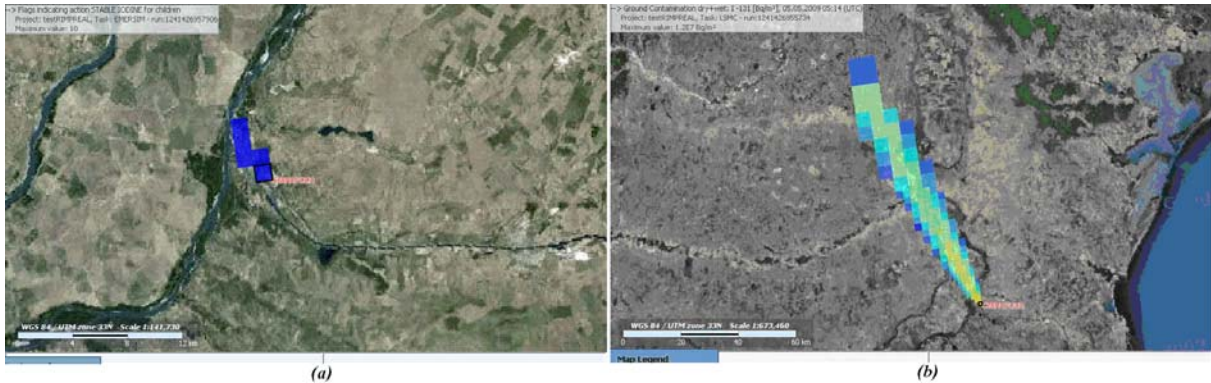


Fig.4. Iodine tablets to children (a); and the ground contamination area (b). RODOS results.

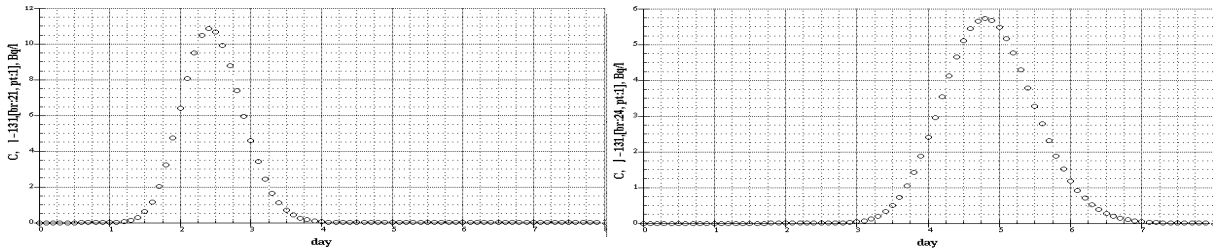


Fig.5. I-131 peak on the Danube, on arrival at Galati (left) and Sulina (right). RODOS results.

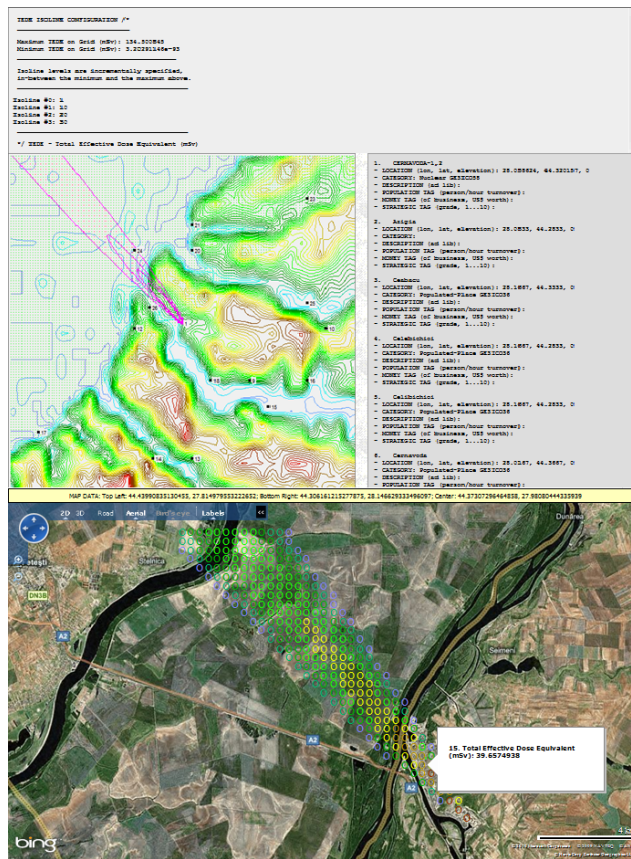


Fig.6. AXIOPOLIS 2009. RAT results.

Figs.4 and Fig.5 exemplify some RODOS results. While Fig.4 follows effects of the radioactive atmospheric release, indicating the area recommended for iodine tablets administration to children, and marking the expanse of the ground contamination area (RODOS), Fig.5 provides information on the I-131 peak arrival at the main towns downstream the Danube river (RODOS), resulting, *inter alia*, in the observation that no drinking water ban would be warranted.

Again, the value of having available an alternative, domestic, toolkit for parallel runs on identical inputs was confirmed. Indeed, IFIN's RAT (*Radiological Assessment Toolkit*) proved to be a welcome convenience to consolidate RODOS results, and increase confidence and the comfort of the analysts and decision makers. Fig.6 is a RAT output clipping.

#### 4. Conclusion

Drill debriefings confirmed: (i) the effective role and weight retained by the extra-academic – civil defence and regulatory - authorities for the decision support systems in the response to abnormal nuclear events; (ii) the complementarity and synergy of major, reference DSSs like RODOS and MOIRA, developed for cross-national compatibility and comparability purposes, on the one hand, and domestic facilities traditionally developed and deployed in vocational research institutions, enjoying the leverage that follows from an organic evolution, responsive to local needs and drawing upon effectively available resources; (iii) the merits of employing expert systems to diminish stress and psychological pressure, avoid confusion or inappropriate decisions in the early phase of emergencies, (iv) the need for a better interface between emergency agencies and stakeholders; and (v) the value of frequent drills in testing the operability of DSSs and identify new desirable features to be added on.

#### Funding

This work was supported by the National Authority for Scientific Research, projects PNCDI-2, 32-117 and PN 09 37 03 01

#### 5. References

1. Rafat M., Raskob W. and Schichtel T. *Concept of outline of the redesigned of RODOS*. EURANOS, CAT-2-TN06-01, Jan 2006, Forschungszentrum, Karlsruhe, Germany, 2006
2. Magan M. and Gallego E. *Application of the MOIRA DSS to evaluate rehabilitation strategies for contaminated freshwater bodies at the local and regional levels*. EURANOS(DEM) – TN(06).,UPM, Spain, 2006
3. Gheorghe A.V., Vamanu D.V. *Disaster Risk and Vulnerability Management From Awareness to Practice*. In *Integrated Risk and Vulnerability Management Assisted by Decision Support Systems*. Adrian V. Gheorgehe, Editor, Springer, 2005



# INDOOR RADON SURVEY IN THE VOJVODINA REGION

S. FORKAPIĆ, N. TODOROVIĆ, I. BIKIT, D. MRDA, J. SLIVKA, M. VESKOVIĆ

*Department of Physics, Faculty of Sciences, University of Novi Sad*

*Trg Dositeja Obradovića 4, 21000 Novi Sad, Serbia*

## ABSTRACT

The results of an indoor radon survey in the Vojvodina region (Serbia) are presented. Long-term average radon measurements in an existing building can be measured relatively simply and inexpensively using a passive device, such as an alpha track detector. Houses in the suburbs were chosen as the target locations of the present investigations. Indoor radon concentrations were measured with CR-39 alpha track detectors at ~1000 locations in Vojvodina during the winter period. Effect of floor level, space under the rooms, boarding and the heating system on radon accumulation are discussed in this paper. For the dwellings typical of such regions, we measure a mean annual radon activity concentration of 112 Bq/m<sup>3</sup> (747 measurements using the alpha track detector CR-39).

### 1. Introduction

Radon is a naturally occurring radioactive gas. It originates from the decay of uranium, which is present in small quantities in all rocks and soils. Radon concentration in soil depends on many physical parameters. The internal soil structure, grain size of soil, type of mineralization and the pore volume determine the value of the emanation coefficient, defined as the fraction of the generated radon that enters the soil pores. It is colorless, odourless and tasteless and can only be measured using special equipment. Because it is a gas, radon can move freely through the soil enabling it to enter the atmosphere. When radon surfaces in the open air, it is quickly diluted to harmless concentrations, but when it enters an enclosed space such as a house, it can sometimes accumulate to unacceptably high concentrations. The regional distribution of radon concentration in buildings is primarily determined by the building materials, the water sources, the domestic gas supplies and in particular by the soil and the geological structures beneath the building. Temperature and pressure differences, wind velocity and humidity also affect the indoor radon concentration. Therefore, the most essential modifying factors are the type of building constructions, the ventilation conditions and the heating and cooling systems.

Measurements of indoor radon are of importance [1] because the radiation dose to the human population due to inhalation of radon and its daughters contributes more than 60% of the total dose from natural sources. Epidemiological studies showed a positive correlation between the cumulative exposure to radon and its progeny and the incidence of lung cancer. It was pointed out that >90% of the dose delivered to the lung comes from the short-lived decay products of radon [2], rather than radon itself.

Many countries worldwide have adopted national reference levels within the range of 200-600 Bq/m<sup>3</sup> as recommended by the International Commission on Radiological Protection [3]. The Serbian Government adopted annual average radon gas concentrations of 200 Bq/m<sup>3</sup> for new houses and 400 Bq/m<sup>3</sup> for old houses as the national Reference Levels above which remedial action to reduce indoor radon in domestic dwellings should be

considered.

This paper deals with the measurements of indoor  $^{222}\text{Rn}$  concentration levels and influences of floor level, space under the rooms, boarding, and the heating system on indoor radon accumulation in the Vojvodina province, situated in the northern part of Serbia.

## 2. Materials and Methods

Long-term average radon measurements in an existing building can be measured relatively simply and inexpensively using a passive device, such as an alpha track detector. Based on previous indoor radon measurements [4],[5] houses in the suburbs were chosen as the target locations of the present investigations. Indoor radon concentrations were measured with CR-39 alpha track detectors at ~1000 locations in Vojvodina during the winter of 2003/2004. Alpha-track detectors are plastics that show microscopic radiation tracks after chemical treatment. We used detectors made of polyallyldiglycol-carbonate (commercially known as CR-39) with dimensions 10 x 10 x 1 mm and sensitivity to alpha particle tracks of 2.9 tracks per  $(\text{cm}^3 \text{ kBq h})/\text{m}^3$ . These detectors were mounted inside small diffusion chambers of plastic with micro-pores of a dimension chosen to prevent the entrance of radon decay products (and usually of thoron,  $^{220}\text{Rn}$ , as well). The exposure time in the closed chambers was 90 d. The etching, evaluating and counting processes were performed by Radosys Company. The plastics were etched by a 25% solution of NaOH for 4 h at a constant temperature of 90°C. The tracks were read and processed by Radosys electronic equipment, which includes a B&W CCD camera and a compatible computer. The results of indoor radon concentration measurements using CR-39 performed from December 2003 to March 2004. Indoor radon activity concentrations have been measured at ~1000 locations in 45 municipalities of the Vojvodina Province. Rooms where people spend most of the time (bedrooms, living rooms) were chosen as measurement locations in flats. The highest radon levels can be expected in basements and ground floors, and measurements at these floors are the most significant for estimation of the radon situation in buildings. The resulting indoor radon levels summarized across administrative regions presented in the radon map of the Vojvodina Province [6].

## 3. Discussion

In the following analysis, we investigate the different factors that can affect annual indoor radon levels. The building characteristics are considered to be the most important factor influencing indoor radon levels. The factors allowing a distinction into subgroups are the type of the house (new or old), space under the rooms, boarding category and floor level on which the living room and bedroom are located. The influence of house type on indoor radon concentration is presented in Fig. 1. However, no differences between old or new types of buildings were found. In further analysis, there is no distinction between "old" or "new" houses. From the analysis of all data, it was found that the indoor radon concentration in 1000 measured houses is significantly higher at the ground floor level than at upper floor levels, as shown in Fig. 2, so the further analysis was performed only for the ground floor of the houses (a total of 747 measurements). The space under the living rooms should be respond to indoor radon level. Of 747 measured houses, a total of 150 have cellars under the living rooms. On the basis of our results, shown in Fig. 3, it is clear that the soil space under the rooms significantly elevates the level of radon activity concentration in the homes because radon directly enters into the rooms from cracks and holes in floors.

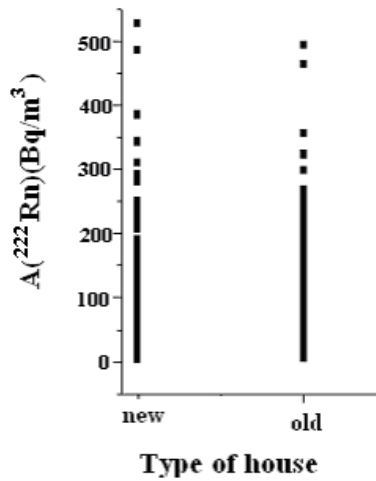


Fig. 1. Influence of type of house on indoor radon activity concentration

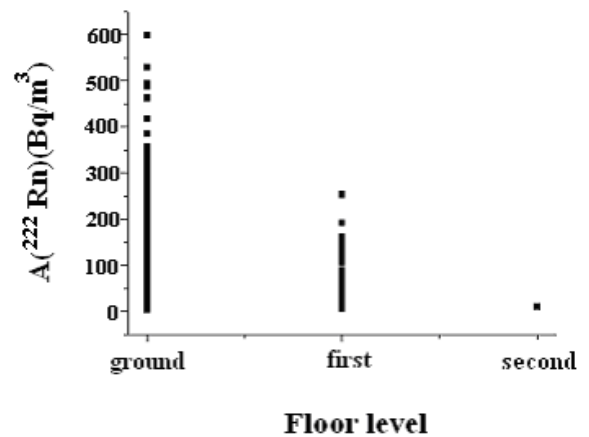


Fig.2. Influence of floor level on indoor radon activity concentration

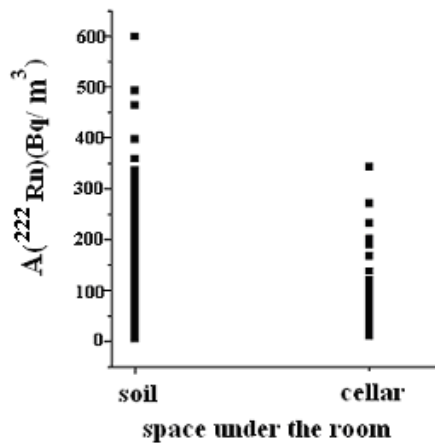


Fig 3. Dependence of indoor radon activity concentration on space under the rooms

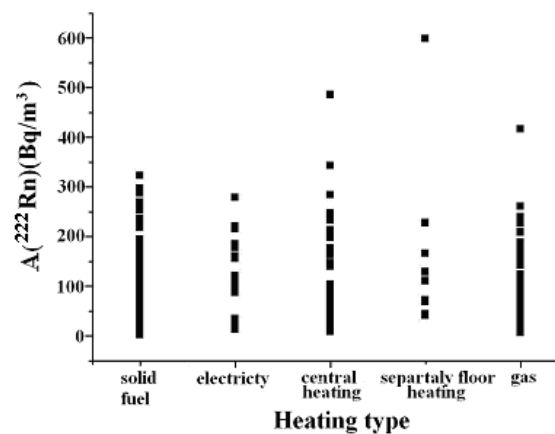


Fig.4. Influence of the heating system on indoor radon concentration in Vojvodina

Some indications of the influence of the heating system installed in the house on indoor radon were also obtained, as shown in Fig. 4. The most frequent type of heating system is solid fuel (298 houses), followed by gas (174), central heating (162), electricity (72), and separately floor heating (41). The maximum value for indoor radon activity concentration ( $599 \text{ Bq/m}^3$ ) is obtained for the separately floor heating. For all types of heating, the recommended levels ( $200 \text{ Bq/m}^3$  for new and  $400 \text{ Bq/m}^3$  for old houses) are exceeded in some houses, but the minimal value is obtained if the electricity is used.

The type of boarding can also affect on indoor radon concentration, as shown in Fig. 5. The maximum value is obtained for wooden boarding. In total 549 houses in our analyses have concrete boarding, 180 houses have wooden floors, and only 18 have soil floors. Figure 9 shows that, in the houses with concrete boarding, the level of indoor radon is less than for those with wooden floors, but in booth cases, the recommended level is exceeded. The porosity of soil boarding possibly contributed to a lower value for indoor radon concentration in respect to the other two board types, though the statistics for this type of board are very poor because of small number of data points.

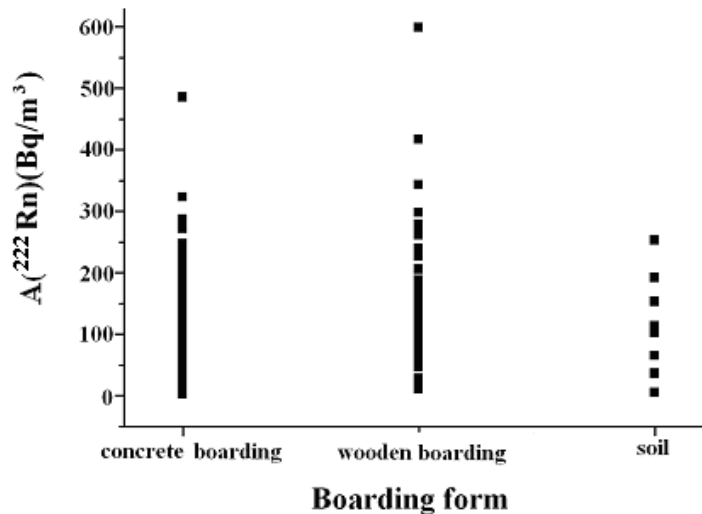


Fig.5. Influence of type of boarding form on indoor radon concentration in Vojvodina

Factors such as a chimney opening in a room, facade material, forced ventilation, hydro isolation, the source of the tap water, surface treatment of interior walls, and wall type of a room could also influence the indoor radon [7], but, in this analysis, we have no data on these parameters.

#### 4. Conclusion

Based on the observed values of indoor radon concentrations, the region of Vojvodina should be ranked as a low natural background radiation area. Almost 20% of the measurements are  $>200$  Bq/m<sup>3</sup> and  $<400$  Bq/m<sup>3</sup>, and 4% of the measurements shown significantly elevated indoor radon concentrations above 400 Bq/m<sup>3</sup>. No influences of building type ("old" or "new") were found. Indoor radon concentration in 1000 measured houses is significantly higher at the ground floor level than at upper floor levels. The soil space under the rooms significantly elevates the level of radon activity concentration in the homes. The minimal value for indoor radon concentration was obtained if the electricity is used as type of house heating. In the houses with concrete boarding, the level of indoor radon is less than for those with wooden floors, but in both cases, the recommended level is exceeded. On the basis of the obtained results, the average indoor activity concentrations of <sup>222</sup>Rn for rural dwellings in the whole province of Vojvodina were calculated (Table 1). The highest observed value of indoor radon concentration in the Vojvodina region is 599 Bq/m<sup>3</sup>, on a ground floor with wooden boards with separately floor heating and soil space under the rooms, in the region of Bela Crkva (Banat district).

Tab 1. Statistics of the measurements of indoor radon concentrations by means of CR-39 during the period December 2002-March 2003 in the Province The Vojvodina (for the ground floor)

No. of measurements	$A_{\text{mean}}$ (Bq/m <sup>3</sup> )	$\sigma A_{\text{mean}}$ (Bq/m <sup>3</sup> )	$A_{\text{min}}$ (Bq/m <sup>3</sup> )	$A_{\text{max}}$ (Bq/m <sup>3</sup> )
747	112	90	1 measured at Plandište	599 measured at Bela Crkva

#### Acknowledgements

The authors acknowledge the financial support of the Ministry of Science and Technological Development of Serbia (project 141002B).

#### Reference

- [1] Martinez, T., Lartigue, J., Navarrete, M., Cabrera, L., Gonzales, P., Ramirez, A. and Elizarraras, V. (1998) Long term equilibrium factor indoor radon measurements, *Journal of Radioanalytical and Nuclear Chemistry*, Vol. 236, No.1-2 231-237.
- [2] United Nations Scientific Committee on Effects of Atomic Radiation, *Ionizing radiation: sources and biological effects* (1982) Exposures to radon and thoron and their decay products. Report to General Assembly with annexes, pp. 141-210.
- [3] The International Commission for Radiological Protection, *Protection against Radon-222 at Home and at Work* (1993) ICRP Publication 65.
- [4] Forkapić, S., Bikit, I., Slivka, J., Conkic, Lj., Veskovic, M., Todorovic, N., Varga, E., Mrdja, D. and Hulber, E. (2007) Indoor radon in rural dwellings of the South-Pannonian region, *Radiation Protection Dosimetry*, Vol. 123, No. 3, pp. 378-383.
- [5] Curcic, S., Bikit, I., Conkic, Lj., Veskovic, M., Slivka, J., Varga, E., Todorovic, N. and Mrdja, D. (2004) The first radon map of The Vojvodina. In: *Proceedings of the 11<sup>th</sup> International Congress of the International Radiation Protection Association*, 23-28 May 2004, Madrid, Spain (paper 6a11 published on CD).
- [6] Bikit, I., Slivka, J., Čonkić, Lj., Krmar, M., Vesković, M., Žikić-Todorović, N., Varga, E., Forkapić, S. and Mrdja, D. (2004) Radioactivity of the soil of The Vojvodina (Northern part of Serbia and Montenegro). *J. Environ. Radioactiv.* 78/1, pp. 11-19.
- [7] Žunić, Z.S., Yarmoshenko, I.V., Birovljev, A., Bochicchio, F., Quarto, M., Obryk, B., Paszkowski, M., Čeliković, I., Demajo, A., Ujić, P., Budzanowski, M., Olko, M., McLaughlin, J.P., Waligorski, M.P.R. (2007) Radon survey in the high natural radiation region of Niška Banja, Serbia, *Journal of Environmental Radioactivity* 92, pp. 165-174.

# SEARCH FOR TENORM SOURCES IN RIVERS SEDIMENTS

N. TODOROVIĆ, I. BIKIT, D. MRDA, S. FORKAPIĆ, J. SLIVKA, M. VESKOVIĆ  
*Department of Physics, Faculty of Sciences, University of Novi Sad  
Trg Dositeja Obradovića 4, 21000 Novi Sad, Serbia*

## ABSTRACT

Possible TENORM pollutants in sediment samples in the Danube, Bega and Tisza Rivers in Serbia were investigated. The radionuclide content of the samples was determined by means of low-level high-resolution gamma-spectroscopy. In addition to the members of the natural radioactive chains of  $^{238}\text{U}$  and  $^{232}\text{Th}$  and the natural  $^{40}\text{K}$ , Chernobyl origin  $^{137}\text{Cs}$  and cosmic origin  $^7\text{Be}$  were detected. It was found that, in comparison with the Danube and Tisza sediment, the Bega sediment is contaminated with  $^{238}\text{U}$  and  $^{137}\text{Cs}$ . The origin of this contamination is discussed. No traces of contamination by nuclear power plants in the region were found, while the presence of technologically enhanced, natural occurring radioactive materials (TENORM) was proved. The higher concentration of  $^{238}\text{U}$  in some locations along the river could be caused by extensive exploitation of phosphate fertilizers in the surrounding agricultural area.

## 1. Introduction

TENORM (Technologically-Enhanced Naturally-Occurring Radioactive Materials) is produced when radionuclides that occur naturally in ores, soils, water, or other natural materials are concentrated or exposed to the environment by activities, such as uranium mining or sewage treatment. Many of the materials that are technically TENORM have only trace amounts of radiation and are part of our everyday landscape. However, some TENORM has very high concentrations of radionuclides that can result in elevated exposures to radiation [1].

The river sediment is considered as a durable and reliable registration of the river pollution by radionuclides, because water pollution components are deposited in the sediment. Long-term radioactive pollution is accumulated and whenever the sediment is mixed up the radionuclides re-enter the ecological nutrition chains [2]. The dislocation of the radionuclides is a very complicated process, but following the logical sense, higher concentration of radionuclides can be expected at locations where the river flow is slowed down. The sediment that is carried into the rivers via the fast flowing tributaries settles in the calmer rivers canals. TENORM pollution enters the canals through scattered point sources (industrial and urban effluent), as well as diffusely along the entire length of the canals (agricultural activity). The contributors of possible radioactive contamination in the Danube, Tisza and Bega rivers sediment in the Vojvodna region in Serbia are in the first place the natural radionuclides concentrated by non-nuclear technologies: coal burning, fertilizing with phosphate fertilizers, and basic chemistry (TENORM). The aftermaths of the atmospheric nuclear tests and the Chernobyl accident, especially  $^{137}\text{Cs}$ , can also be accumulated in the canal sediment. In principle, nuclear power plants operating in the region ((Paks, Krško, Cernavoda, Kozloduj) can also contaminate the canals by atmospheric emission.

## 2. Sampling and measurement methods

Samples were taken from several locations of the Danube, Tisza and Bega rivers canals, Fig 1. The wet sample mass taken for radioactivity analysis was about 1 kg. The sediment samples were prepared by drying at  $105\text{ }^{\circ}\text{C}$  to a constant mass. After homogenization, they were transferred to sample holders, cylindrical containers (67mm diameter and 62mm

height), and sealed. The radionuclide content of the samples was measured by means of the reversed electrode “GMX” type HPGe spectrometer made by ORTEC. The nominal efficiency of the detector is 32% and the resolution is 1.9 keV. This detector has a thin dead layer on the outer surface and a beryllium entrance window that enables detection of gamma rays below 100 keV with excellent efficiency. The detector was operated inside the 25 cm thick iron shield made from pre-World War II cast iron. The radon level in the measuring room was kept constant and low ( $<10 \text{ Bq/m}^3$ ) by forced ventilation. The integral background count rate of the shielded detector was less than 1.5 counts per second. The detector was calibrated by means of a reference radioactive material in cylindrical geometry (NBS Standard Reference Material 4350B) [3]. The reference material (river sediment) and the samples were measured in the same geometry. Self-absorption effects due to slightly different densities were taken into account using the ANGLE computer code based on the concept of the effective solid angle. Such careful calibration was necessary in order to ensure low calibration error ( $<10\%$ ) in the low-energy region (below 100 keV) where the strongest analytical lines of  $^{234}\text{Th}$  (direct  $^{238}\text{U}$  descendant) are located. The typical sample measurement time was about 50 ks. A modified version of the SAMPO program was used to process the spectra in such a way that it always calculated specific activities of 21 selected nuclides. The selection list includes all relevant natural radionuclides and long-lived fission and corrosion products. The program calculates the activity concentration of an isotope from all prominent gamma lines after peaked background subtraction. This approach, yielding maximum statistical accuracy and safe isotope identification, needs a comment on the calculated activity of radioactive chains. The activity of  $^{238}\text{U}$  was determined as a weighted mean of  $^{234}\text{Th}$  and  $^{234\text{m}}\text{Pa}$  activities, which are equal within measurement uncertainties. The issue of  $^{238}\text{U}/^{234}\text{Th}$  equilibrium is settled by our recent investigations [4]. The  $^{235}\text{U}$  activity concentration was obtained by subtracting the  $^{226}\text{Ra}$  contribution from the area of the 186 keV gamma line, as well as from the lines of  $^{235}\text{U}$ ,  $^{227}\text{Th}$ , and  $^{223}\text{Ra}$ , with all values in fair agreement with the supposed equilibrium. All measurement uncertainties are presented at 95% confidence level [4].

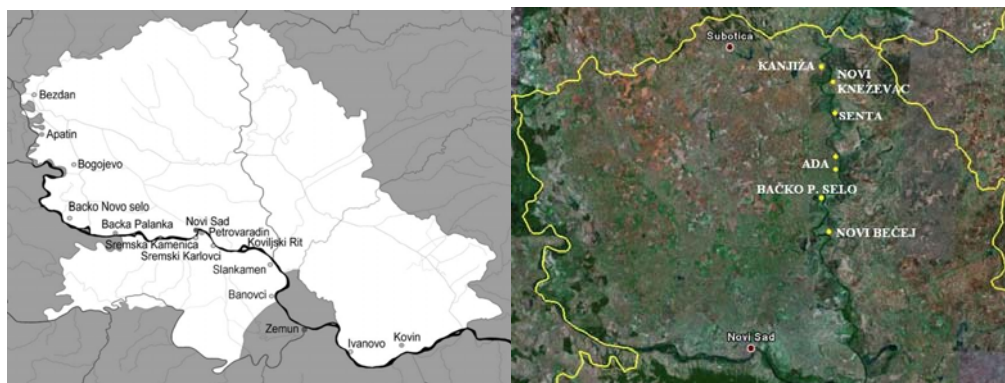


Fig 1. Map of sediment sample locations along the Vojvodina section of the Danube and Tisza River in Serbia

### 3. Results and analysis

In Table 1 the comparison of the Danube, Bega and Tisza sediment results with the recent results agricultural soil [5] is presented. Activity concentrations of  $^{226}\text{Ra}$ ,  $^{232}\text{Th}$ , and  $^{40}\text{K}$  are roughly the same within statistical variations in all the three media. However, the mean  $^{137}\text{Cs}$  activity concentration is 1.6 times greater in the Bega than in the Danube sediment, 6.8 times greater than in Tisza sediment and 3.7 times greater than in the typical Vojvodina soil are due to a time lag (two years from Bega measurements, and four years from Danube). The dominant contributor of the  $^{137}\text{Cs}$  contamination is the Chernobyl accident in 1986.

$^{238}\text{U}$  activity concentrations is almost two times higher in Bega sediment than in Tisza, and is almost equal for the Tisza and Danube, coming from phosphate fertilizers or detergents [5]. The activity concentrations of natural radionuclides  $^{226}\text{Ra}$ ,  $^{232}\text{Th}$ , and  $^{238}\text{U}$  are expected. The results obtained on  $^{226}\text{Ra}$  and  $^{238}\text{U}$  activity concentrations [6] prove the absence of depleted uranium (DU) from the sediments. Activity concentrations of all fission and corrosion products were found to be below detection limits. This means that the operation of several nuclear power plants in the region did not cause any measurable contamination of the canal sediment. In order to trace the sources of the contaminants, we analyzed the variation of  $^{137}\text{Cs}$ ,  $^{238}\text{U}$ , and  $^{232}\text{Th}$  activity concentrations (Fig. 2). The rather uniform  $^{232}\text{Th}$  distribution proves its natural origin.

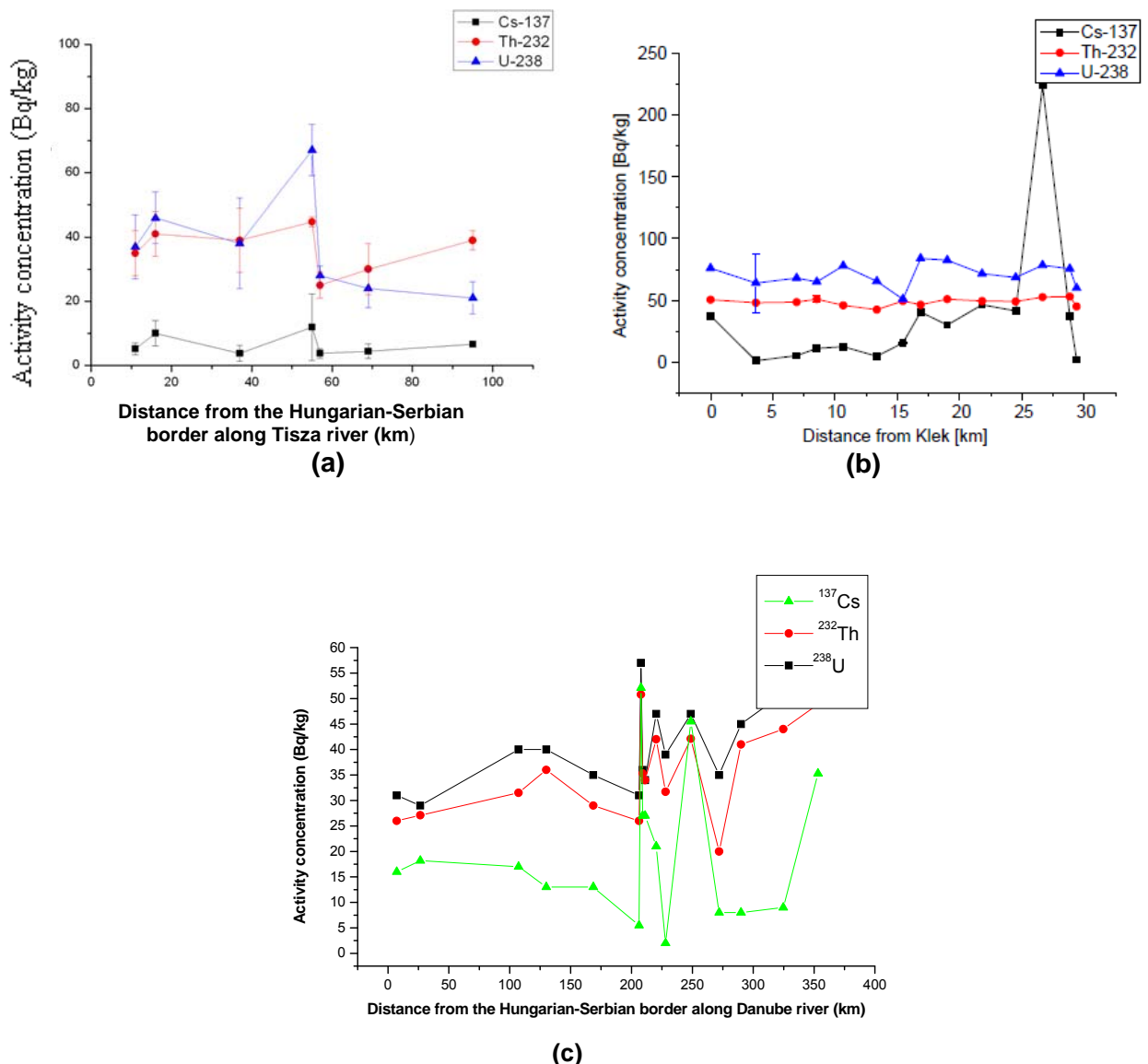


Fig. 2. Variation of the  $^{137}\text{Cs}$ ,  $^{232}\text{Th}$ , and  $^{238}\text{U}$  activity concentrations (mean values of top and bottom sediment) along the (a) Tisza, (b) Bega and (c) Danube canal. Lines connecting data points are only meant to guide the eye.

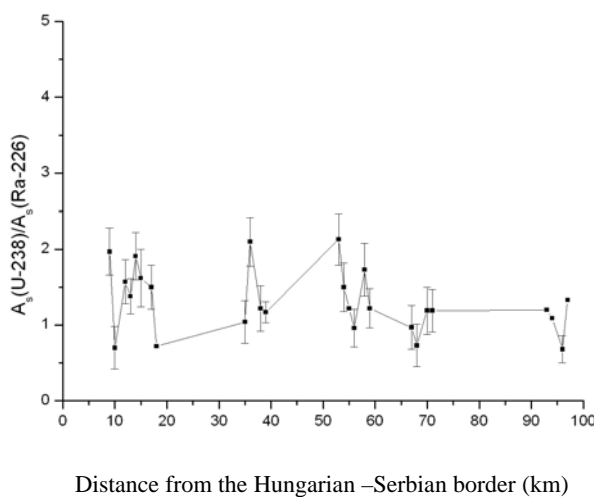
Assuming radioactive equilibrium in sediment, the proportion  $A(^{238}\text{U})/A(^{226}\text{Ra})$  should be about 1.  $^{226}\text{Ra}$  is particularly important as a source of NORM (Naturally Occurring Radioactive Materials), radium is soluble and may readily leach from soils and form compounds that can be taken up by plants and animals and is thus metabolized by both



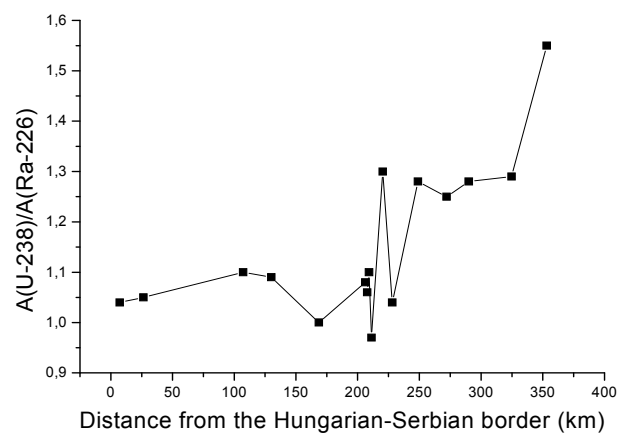
plants and animals. The  $A(^{238}\text{U})/A(^{226}\text{Ra})$  proportion is shown on Fig 3 (every point denote one sediment sample). The  $A(^{238}\text{U})/A(^{226}\text{Ra})$  proportion along rivers is enhanced and for the many samples the ratio is higher then 1 (especially in Bega and Tisza rivers), which is different from the natural ratio [5]. Having in mind that  $^{226}\text{Ra}$  is daughter nucleus of  $^{238}\text{U}$ , these results indicate contamination with  $^{238}\text{U}$ . The  $^{235}\text{U}/^{238}\text{U}$  activity ratio in Tisza sediment is in good agreement with the natural value [4], the contaminant is probably the natural  $^{238}\text{U}$ . The higher concentration could be caused by extensive exploitation of phosphate fertilizers in the surrounding agricultural area (TENORM).

Tab 1: Comparison of activity concentration data in the Danube, Bega and Tisza sediment and in agricultural soil in the Vojvodina region .

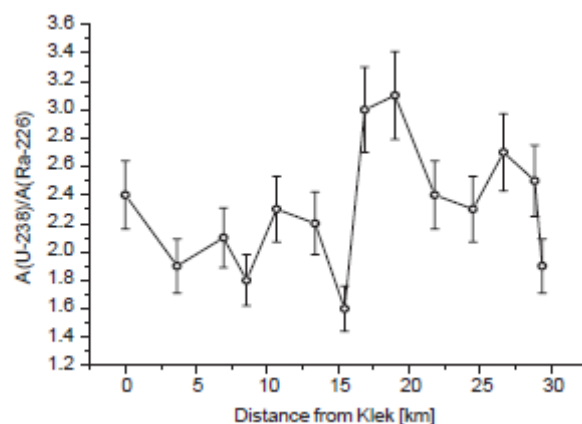
Radionuclide	$\bar{A}$ (Bq/kg) Danube	$\bar{A}$ (Bq/kg) Bega	$\bar{A}$ (Bq/kg) Tisza	$\bar{A}$ (Bq/kg) agricultural soil
$^{40}\text{K}$	$445 \pm 88$	$520 \pm 48$	$486.5 \pm 20.7$	554
$^{137}\text{Cs}$	$28 \pm 23$	$45 \pm 7.4$	$6.6 \pm 0.6$	12
$^{226}\text{Ra}$	$32 \pm 8$	$30 \pm 3$	$27.7 \pm 2.7$	39
$^{232}\text{Th}$	$36 \pm 9$	$49 \pm 4$	$36.5 \pm 5.0$	53
$^{238}\text{U}$	$42 \pm 12$	$71 \pm 15$	$37.3 \pm 7.3$	51



(a)



(b)



(c)

Fig 3. The  $A(^{238}\text{U})/A(^{226}\text{Ra})$  proportion in (a) Tisza and (b) Danube and (c) Bega sediment (every point denote one sediment sample). Lines connecting data points are only meant to guide the eye.

#### 4. Conclusion

Comparing the radionuclide activity concentration for the Bega canal sediment with the the Danube and Tisza sediment and Vojvodina soil, it is shown that the Bega canal sediment contains significantly elevated levels of  $^{137}\text{Cs}$  and  $^{238}\text{U}$ .  $^{137}\text{Cs}$  originates mostly from the accident of the nuclear power plant in Chernobyl in 1986. Due to its long half-life (30.2 y), it was relocated, washed out and redistributed, but is still present in the Vojvodina reach of the Danube, Bega and Tisza rivers. Large differences between the minimum and maximum  $^{137}\text{Cs}$  activity concentrations at a given location show typical features of a man-made contaminant. Some materials with a high  $^{238}\text{U}/^{226}\text{Ra}$  ratio (phosphate fertilizers, sodium tripoliphosphate) are identified as contributors of  $^{238}\text{U}$  contamination. No traces of contamination by nuclear power plants in the region in Danube, Tisza and Bega sediments were found. Some TENORM problems which emerged in the present work is probably from the phosphate fertilizers.

#### Acknowledgment

The authors acknowledge the financial support of the Ministry of Science and Technological Development of Serbia, within the project Nuclear Spectroscopy and Rare Processes (no.141002B)

#### References

- [1] Evaluation of Guidelines for Exposures to Technologically Enhanced Naturally Occurring Radioactive Materials, Committee on Evaluation of EPA Guidelines for Exposure to Naturally Occurring Radioactive Materials, National Research Council, ISBN: 0-309-58070-6, 1999
- [2] Aarkrog, A., Trapeznikov, A.V., Molchanova, I.V., Yushkov, P.I., Pozolotina, V.N., Polikarpov, G.G., Dahlgard, H., Nielsen, S.P., 2000. Environmental modelling of radioactive contamination of floodplains and surlakes along the Tеча and Iset rivers. *J. Environ. Radioactiv.* 49, 243.
- [3] Varga, E., Bikit, I., Mrda, D., Slivka, J., Zikic-Todorovic', N., Curcic, S., Veskovic, M., Conkic, Lj., 2003a. Calibration of GMX HPGe detector with NBS reference source. *Proceedings of the BPU-5*, vol. A-58, pp. 2367
- [4] Bikit, I., Mrda, D., Todorovic, N., Varga, E., Forkapic, S., Veskovic, M., Slivka, J., Conkic, Lj., 2004. Possibility of prompt  $^{238}\text{U}$  determination by gamma-spectroscopy. *Jpn. J. Appl. Phys.* 44, 377–379.
- [5] Bikit, I., Slivka, J., Conkic, Lj., Krmar, M., Veskovic, M., Zikic-Todorovic, N., Varga, E., Curcic, S., Mrda, D., 2004. Radioactivity of the soil in Vojvodina (Northern province of Serbia and Montenegro). *J. Environ. Radioactiv.* 78/1, 11–19.
- [6] Bikit, I., Slivka, J., Mrda, D., Zikic-Todorovic N., Curcic, S., Varga, E., Veskovic, M., Conkic, Lj., 2003. Simple Method for Depleted Uranium Determination, *Jpn.J.Appl. Phys.*, Vol.42, pp. 5269-5273

# 6 MEV LINAC PHOTON SPECTRA RECONSTRUCTION BASED ON A MIXED EXPERIMENTAL-MONTE CARLO SCATTER ANALYSIS TECHNIQUE

B. JUSTE, R. MIRÓ, G. VERDÚ

*Institute for Industrial, Radiophysical and Environmental Safety (ISIRYM). Universitat Politècnica de València. Camí de Vera s/n. 46022. Valencia. Spain*

S. DíEZ, J. M. CAMPAYO

*Hospital Clínic Universitari de Valencia. Avda. Blasco Ibáñez, 17, 46010, Valencia. Spain.*

## ABSTRACT

This work is centred in calculating the primary photon spectrum of a linear accelerator by means of a scatter analysis methodology. The developed technique consists on irradiating the centre of a PMMA block located at 100 cm distance from surface and measuring at five specific positions, the scattered photons and electrons emitted after hitting the plastic with different scatter angles. The transport of mono-energetic beams has been simulated with the MCNP5 Monte Carlo code in order to register the scatter contribution caused by the attenuator. These ionization experimental values along with the simulated results, allow calculating the original spectrum as the sum of mono-energetic individual energy bins using the *Schiff* Bremsstrahlung model. We present this theory to calculate a 6 MeV photon beam from an *Elekta Precise* radiotherapy unit utilizing the gradient of depth dose measurements in a water tank. Relative depth and profile dose curves calculated in a water phantom using the reconstructed spectrum agree with experimentally measured dose data to within 3%.

## 1. Introduction

The study of X-ray and photon spectra reconstruction is extremely important for quality control of radiographic diagnostic systems and linear accelerators. Moreover, the photon energy spectrum is necessary when establishing a radiotherapy treatment planning system for a medical linear accelerator (*linac*). The pulsed and intense nature of these beams makes the direct measurement of their energy spectra complicated in clinical applications because of the high photon fluence rates in an extremely short period of time that cause significant detector photon pile-up and detector saturation.

Therefore, an alternative way of calculating the beam photon spectra of a linear accelerator based on indirect measures has been performed [1].

We have focused our work in this kind of reconstruction method since the necessary equipment has been easily available at the *Hospital Clínic Universitari de València* and it provides independent confirmation of source models for a given machine.

This spectrum reconstruction methodology involves measuring the dose in an ionization chamber after the beam passes through an attenuator.

Concretely, the scattering at different energy bins in various scattering angles produced after a photon beam goes through a plastic block is analyzed.

Since Compton scattering is the preponderance interaction in the radiotherapy usual energy ranges, it can be stated that the scatter analysis will be mainly centred in the number of photon Compton scatter interactions in different energy bins that the primary spectrum generates at a specific angle when the beam come into contact with the scatterer.

## 2. Methods and materials

## 2.1. The Schiff Bremsstrahlung model

The mathematical procedure to develop the spectral reconstruction is to apply the *Fredholm* integral equation of the first kind [2]. This equation is a well known example of a linear ill-posed problem. To solve it, a non-iterative stabilized approximation technique, called the regularization method, can be applied.

Photon beams are produced by Bremsstrahlung after electrons hit the target placed on the linac head. The relative photon particle fluence at a specific photon energy  $k$ , can be expressed using the parametric version of the *Schiff* [3] formula:

$$\Phi(k, T, t) = (1/k) \left[ \left( 1 - \frac{k}{T} \right) (\ln \eta - 1) + \left( \frac{k}{T} \right) (\ln \eta - 0.5) \right] \exp(-\mu_t(k)t) \quad (1)$$

In equation (1),  $T$  is the total energy of electron incident on the target in MeV, and  $t$  the hypothetical thickness of target material equivalent in attenuation to the entire filtering system (target, flattening filter, etc) and  $\mu_t(k)$  is the total linear attenuation coefficient for the target's material at energy  $k$ , extracted from NIST database tables.

$$\eta = \left[ \left( \frac{0.511k}{2T(T-k)} \right)^2 + \left( \frac{Z^{1/3}}{111} \right) \right]^{-1/2} \quad (2)$$

In equation (2),  $Z$  makes reference to the effective atomic number for all attenuating materials, taken here as target atomic number. And, 111 is a constant calculated and offered by *Schiff*.

It is then necessary to experimentally find accurate values for the free parameters  $T$  and  $t$  in the parametric spectral model of equation (1) in order to determine the spectrum.

## 2.2. Spectrum reconstruction method

For the spectral reconstruction, we have used five measurements taken at five different scattering angles from the central axis.

The unknown spectrum has been divided into 350 energy bins (0.02MeV, 0.04MeV, 0.06 MeV, ..., 7 MeV). The five different exact positions of the ionization chamber are detailed in the figure 1.

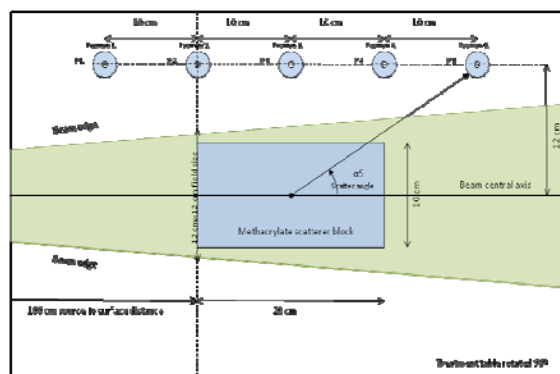


Fig 1. Top view of the experimental procedure for scatter measurement at five different ionization chamber positions.

The MCNP5 code is used to simulate the procedure scheme detailed in figure 1.

The model including the ionization chamber located in  $P1$  (position 1), offers the estimation of  $a1$ , the relative magnitude of the scatter signal per photon exiting the accelerator's head for a mono-energetic beam at first energy bin (0.02MeV).

Likewise,  $a2$  is calculated for the second energy bin (0.04MeV), until  $a350$  for the last bin (7 MeV) is obtained.

We can state then that calculated  $[a1, a2, . . . , a350]$  quantities are the relative mono-energetic scatter signals for  $P1$ .

Let  $[x1, x2, . . . , x350]$  represent the unknown number of photons in each bin of our unknown spectrum, expressed each parametrically by equation (1).

The scatter signal  $P1$  measured at position 1 is the sum of the scatter signals contributed by each individual bin:

$$\begin{aligned}
 P1 &= a_1 \cdot x_1 + a_2 \cdot x_2 + \dots + a_{350} \cdot x_{350} \\
 P2 &= b_1 \cdot x_1 + b_2 \cdot x_2 + \dots + b_{350} \cdot x_{350} \\
 P3 &= c_1 \cdot x_1 + c_2 \cdot x_2 + \dots + c_{350} \cdot x_{350} \\
 P4 &= d_1 \cdot x_1 + d_2 \cdot x_2 + \dots + d_{350} \cdot x_{350} \\
 P5 &= e_1 \cdot x_1 + e_2 \cdot x_2 + \dots + e_{350} \cdot x_{350}
 \end{aligned}
 \tag{3}$$

Where  $[P1, P2, P3, P4, P5]$  are the experimental measured scatter signals for positions 1 to 5. Replacing  $[x1, x2, . . . , x350]$  by their parametric forms given in equation (1), we can solve the system (Eq. 3) where the only unknowns are  $T$  and  $t$  using the ionization method. Once these are determined, the spectrum is given by equation (1).

### 3. Experimental Procedure

The experimental procedure scheme can be observed in Figure 1. This figure shows the experimental set-up developed to measure the ionization charge at different scatter angles around the plastic and use these data for primary spectral reconstruction.

Measures have been made with the Gantry rotated 90°. The scattering plastic is placed at a standard 100 cm distance from the source target and the horizontal beam's isocentre fits the centre of the plastic surface. A *Scanditronix* ionization chamber Farmer FC65-P cylindrical ionization chamber with a 0.65 cm<sup>3</sup> sensitive volume with build-up is placed at five different specific positions outside of the primary beam ( $P1, P2, P3, P4$ , and  $P5$ ) with the aim of measuring secondary photons charge produced by the scatterer in these locations.

The attenuator plastic consists of a Methacrylate rectangular prism of 20 cm long x 10 cm x 10 cm. We used a 12 cm x 12 cm field size at isocentre in order to cover completely the scatterer block.



Figure 2. View of the *Elekta* linac upper head for 6 MeV X-ray beams and the water phantom.

To obtain the ionization in the chamber due to secondary photons it is necessary to obtain two measures with the same quantity of linac monitor units delivered in each one. The first reading is taken without the plastic scatterer in order to measure the background signal (taking into consideration the jaw transmission, scatter off the room walls and floor and

accelerator head leakage). On the other hand, to obtain the second one, the ionization chamber stays at the same location, placing the plastic scatterer in the isocentre beam axis. The contribution from secondary photons produced in the scatterer is calculated by subtracting the first reading from the second.

Figure 2 shows the *Hospital Clinic Universitari de València* radiotherapy treatment room where the *Elekta Precise* linear accelerator is placed, and the experimental set-up developed.

## 4. Monte Carlo Simulations

### 4.1. Simulation of scattered mono-energetic ionization detection

The Monte Carlo simulation allows registering the energy at a specific ionization chamber location when a photon mono-energetic beam from a specific energy bin of the spectrum is emitted.

We have used the MCNP, version 5 [4] Monte Carlo computer code to register each energy bin charge according to the geometry described in Figure 1.

To obtain these data, the full *Elekta* linac head didn't need to be modelled. Just a point source irradiating the plastic scatterer and the ionization chamber placed at different locations were modelled.

The photon energy cut-off considered for this study has kept the default value in MCNP, 1 keV. An electron energy cut-off of 0.1 MeV has been selected.

The tally used to estimate detector signal has been the \*F8:P,E, the pulse-height distribution in the detectors modified to energy units.

Each simulation run follows the transport of 100 million histories particles, in order to obtain a statistical error always below the 5%.

It has been necessary executing 1750 simulations to obtain data from (*a1*, ...*a350*) to (*e1*, ...*e350*). Given the high amount of simulations needed, which means an extremely long time calculation, the MCNP code has been parallelized in an SGI Altix 3700, using the MPI parallel protocol with 16 processors. We have also increased MCNP5 calculation speed by recompiling the code using the -O2 optimization option of the Intel Fortran Compiler 9.0, on the Linux parallel computing machine, which enables optimizations for speed.

### 4.2. Simulation of the accelerator head

The simulation of the whole unit is required for the final stage of the work, where the reconstructed spectrum needs to be validated.

To simulate the transport of electrons and photons that travel through the unit, from the source up to the detector located at the water phantom, we have realistically modelled the geometry of all the components.

The *Elekta Precise* linear accelerator head has been represented by the target disc, primary collimators, flattening filter, the ion chamber assembly and the auto-wedge assembly which includes the wedge and the backscatter plate. All dimensions and materials have been specified by the manufacturer.

To characterize the source particles, these simulations have used the 6 MeV reconstructed photon spectrum calculated in the first stage of the work, setting a 10 cm × 10 cm field size.

The source was positioned at a distance of 100 cm from a water phantom whose volume was 50 cm × 50 cm × 50 cm.

The FMESH4 tally, associated with its respective flux-to-dose conversion factors, has been used in this case to register dose distribution inside the water phantom.

## 5. Results and Conclusion

To validate the reconstructed spectrum, two systems have been applied. One of them consists of comparing the 6MeV energy spectrum with another spectrum provided by *Sheikh-Bagheri and Rogers* [6].

The maximum difference between both spectrums was found to be 7%.

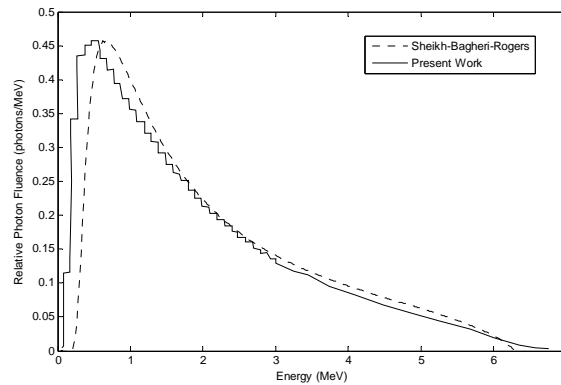


Fig. 4. Comparison of this work reconstructed photon 6MeV spectra and the one provided by Sheikh-Bagheri and Rogers.

To complete the reconstructed spectrum validation, the other system applied was based on using Monte Carlo simulations to calculate relative depth dose curves at a water phantom. The calculated percentage depth-dose data at the central axis beam for standard clinical conditions derived from the reconstructed spectrum were found to agree with experimental measurements to within approximately 1%.

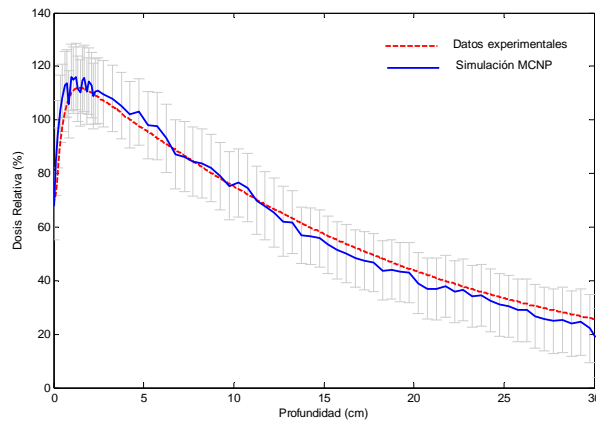


Figure 5. Relative depth dose comparison.

This comparison offers a good agreement between measured and calculated depth dose values, reflecting the accuracy of the reconstructed spectra method developed in this work. Considering the results obtained, we can state that the scatter reconstruction methodology is an accurate method for X-Ray spectral calculation.

## References

- [1] A. Nisbet, H. Weatherburn, J. D. Fenwick and G. McVey, "Spectral reconstruction of clinical megavoltage photon beams and the implications of spectral determination on the dosimetry of such beams" *Phys. Med. Biol.* 43, 1998, pp 1507–21.
- [2] G. L. Karakostas and P. Ch. Tsamatos, "Multiple positive solutions of some Fredholm integral equations" *Electronic Journal of Differential Equations*, Vol. 2002(2002), No. 30, pp. 1-17.
- [3] G. E. Desobry and A. L. Boyer. "Bremsstrahlung review: An analysis of the Schiff spectrum". *Med. Phys.*, vol. 18, 1991, pp. 497–505.
- [4] X-5 MONTE CARLO TEAM, "MCNP – A General Monte Carlo NParticle Transport Code, Version 5", LA-UR-03-1987, Los Alamos Nacional Laboratory, April 2003.
- [5] D. [Sheikh-Bagheri](#) [D. W. O. Rogers](#), "Monte Carlo calculation of nine megavoltage photon beam spectra using the BEAM code" *Medical Physics* , March 2002, Volume 29, Issue 3, pp. 391-402.

# WEB BASED DOSIMETRY SYSTEM FOR READING AND MONITORING DOSE THROUGH INTERNET ACCESS

SC PERLE, K BENNETT, J KAHILAINEN, M VUOTILA

*Mirion Technologies, USA & Finland*

## Immediate Readings Of Radiation Dose Online

The instadose™ dosimeter from Mirion Technologies is a small, rugged device based on patented direct ion storage technology and is accredited by the National Voluntary Laboratory Accreditation Program (NVLAP) through NIST, bringing radiation monitoring into the digital age. Smaller than a flash drive, this dosimeter provides an instant read-out when connected to any computer with internet access and a USB connection. Instadose devices provide radiation workers with more flexibility than today's dosimeters.

## The Technology

Non Volatile Analog Memory Cell surrounded by a Gas Filled Ion Chamber. Dose changes the amount of Electric Charge in the DIS Analog Memory. The total charge storage capacity of the memory determines the available dose range. The state of the Analog Memory is determined by measuring the voltage across the memory cell.

Table1. Technical Specifications

Wear Location	Collar or upper torso
Minimum Reportable Dose	0.01 mSv (1 mrem)
Lower Limit of Detection	0.01 mSv (1 mrem)
Useful Dose Range	0.01 mSv - 5 Sv (1 mrem - 500 rem)
Energy Response	Photon 15 keV - 6 MeV



Figure1. Linearity results

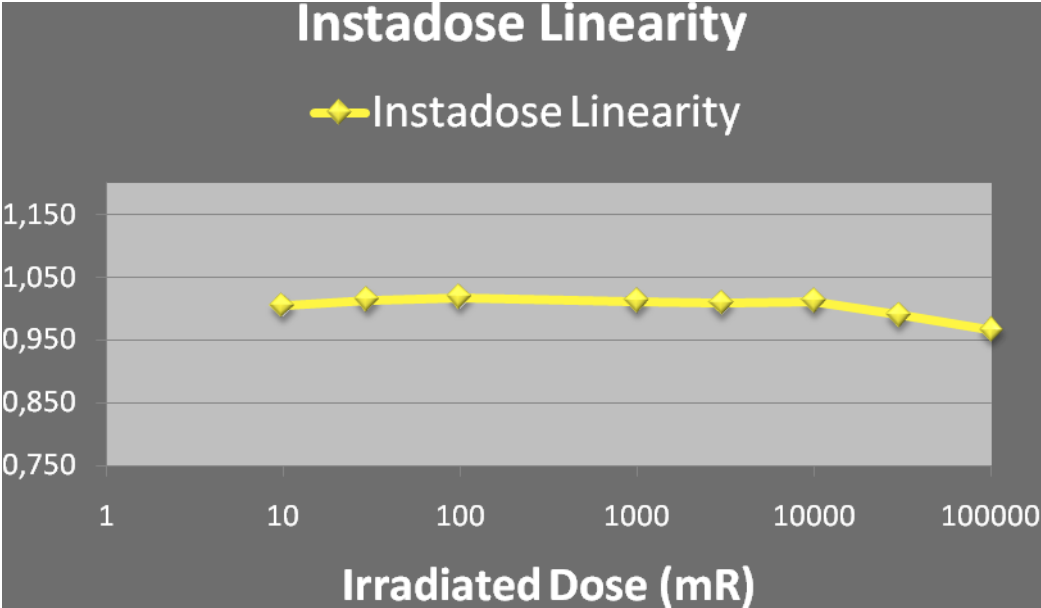


Figure2. Angularity results

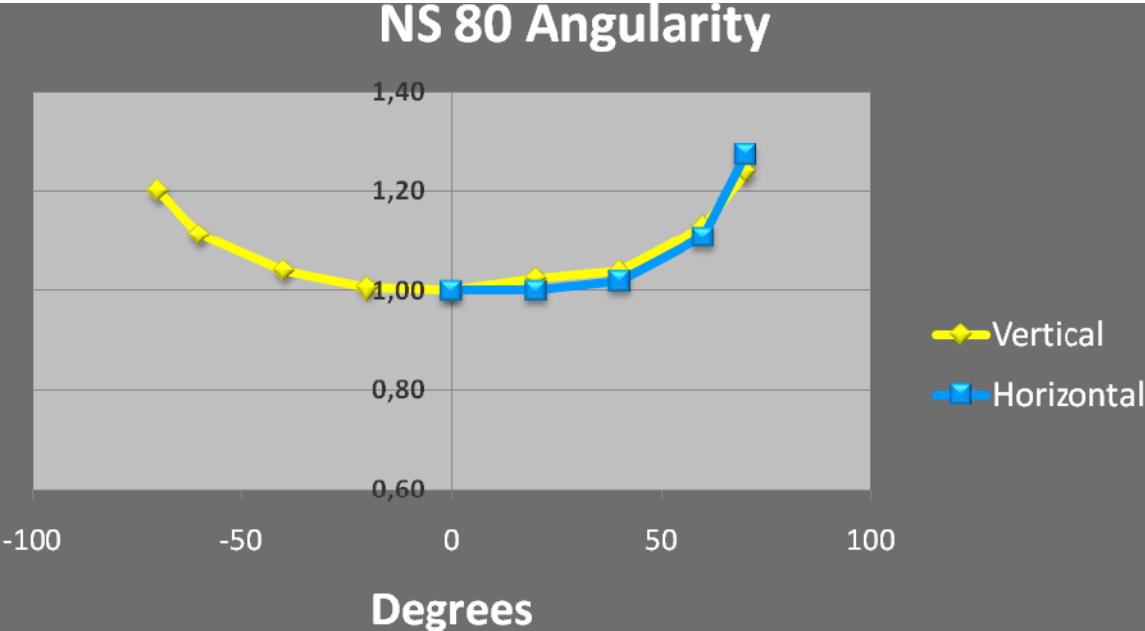
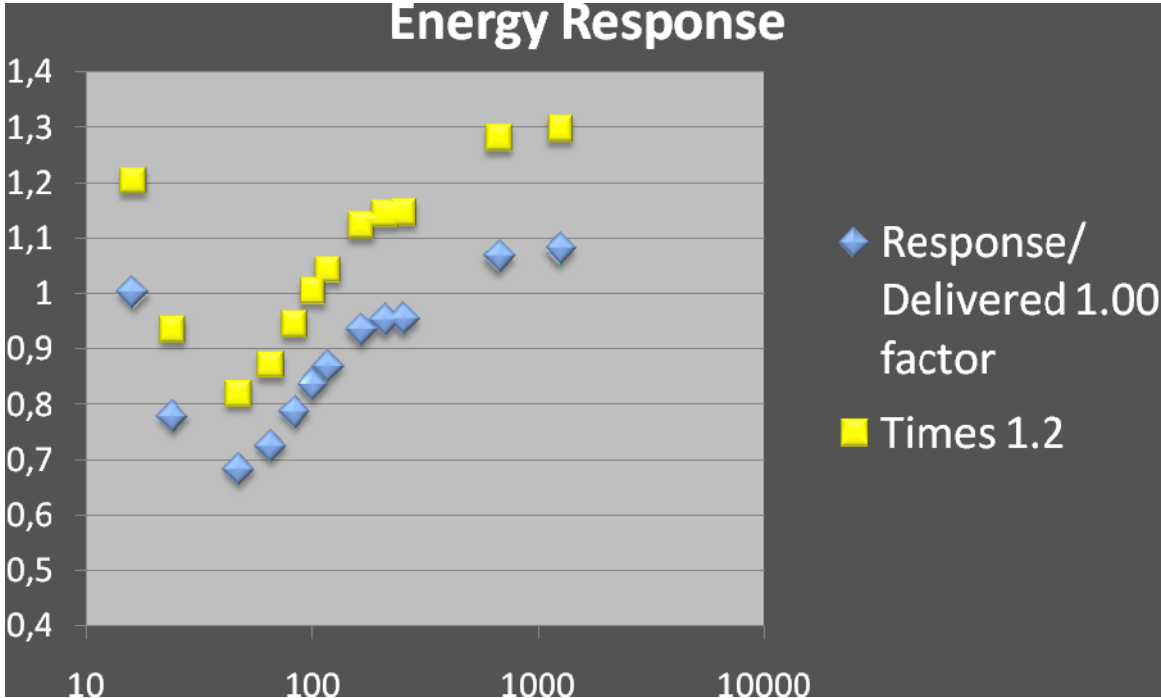


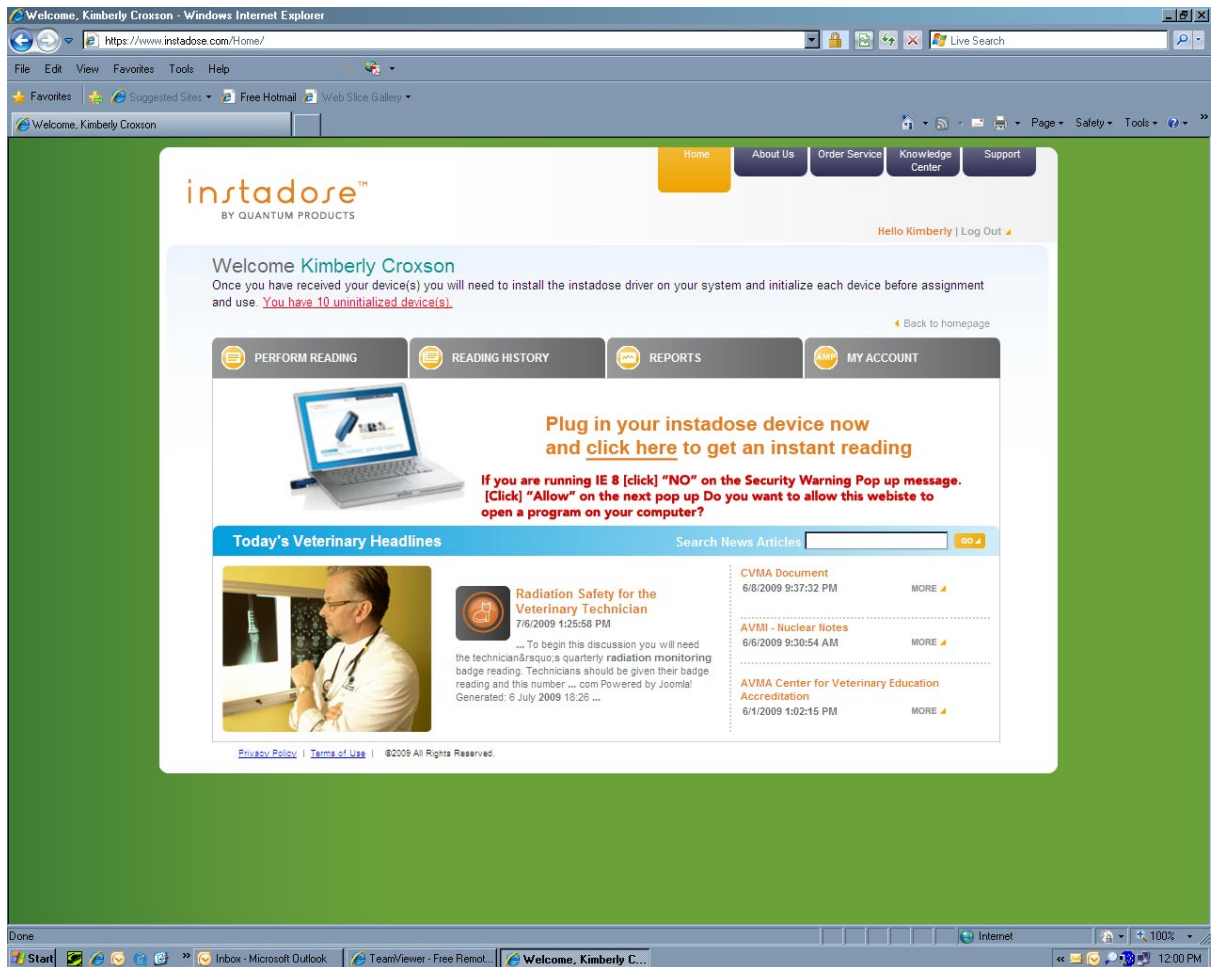
Figure3. Energy Response. Energy Response can be customized to the facility.



**The Software**

AMP(Account Management Program) provides secure real time access to account details, device assignments, reports and all pertinent account information. Access can be restricted based on the role assignment assigned to an individual. A variety of reports are available for download and customizing.

Figure4. Screen shot of the webpage.



## The Advantages of the instadose dosimeter

- Unlimited reading capability

- Concerns about a possible exposure can be addressed immediately
- Re-readability without loss of exposure data, with cumulative exposure maintained

Figure5. How the device opens



Figure6. Available colors





EUROPEAN NUCLEAR SOCIETY

Rue Belliard 65, 1040 Brussels, Belgium  
Telephone +32 2 505 30 54, Fax + 32 2 502 39 02  
[enc2010@euronuclear.org](mailto:enc2010@euronuclear.org) - [www.euronuclear.org](http://www.euronuclear.org)

